Contents lists available at ScienceDirect

Solid State Nuclear Magnetic Resonance

Isomorphism and disorder in o-chlorohalobenzenes studied by NQR

Silvina C. Pérez*, Alberto Wolfenson [1], Mariano Zuriaga [1]

Facultad de Matemática, Astronomía y Física, Universidad Nacional de Córdoba, IFEG – CONICET, Medina Allende s/n, Ciudad Universitaria, 5000 Córdoba, Argentina

ARTICLE INFO

ABSTRACT

In this work we present experimental results that allow to characterize different solid modifications found in o-chlorohalobenzenes. Three disordered phases have been found in o-chlorobromobenzene. The stable phase at high temperature (phase I) is also obtained by quenching the sample at 77 K. Slow cooling allow to obtain the low temperature phase III which, on heating, transforms to phase II at 183 K and this, in turns, transforms to phase I at $T \sim 210$ K. The disorder evidenced through the Nuclear Quadrupole Resonance spectra, is attributed to a random occupation of chlorine and bromine sites. In all phases there is evidence of molecular reorientations out of the benzene ring plane around the pseudo-symmetry axis between the atoms of Cl and Br. In o-chlorofluorobenzene two phases have been found depending on the cooling rate. One phase is disordered due to the random exchange of the occupation of Cl and F sites. In this case, there is also evidence of molecular reorientations out of the benzene ring plane, but in this case the reorientation is around the pseudo-symmetry axis that pass through the C–Cl bonds. Comparisons with the behavior of o-dichlorobenzene are also made.

1. Introduction

The majority of organic compounds have the ability to exist in more than one crystal structure or phase that have different arrangements or conformations of the molecules in the crystal lattice, an ability which is known as polymorphism. Monotropic modifications of the same substance are most frequently encountered. For a monotropic system, the free energy curves do not cross, and therefore no reversible transition can be observed below the melting point. Controlling the formation of different polymorphs is still a challenge in crystal engineering and thus, different polymorphs are found randomly. Among the polymorphs, there are those with a certain disorder in the molecular arrangement including rigid disorder. Typical examples of this kind of disorder are p-chlorobromobenzene and p-chloroiodobenzene, which are isomorphous with p-dichlorobenzene and the average molecule is obtained by centrosymmetric superposition of two molecules with half-weight atoms [1–3].

With the aim of finding if the disorder and isomorphism present in p-chlorohalobenzenes is also present in o-chlorohalo-benzenes, three compounds of the chlorobenzene derivatives o-C_6H_4ClX (X=Br, Cl, F) have been studied using ^{35}Cl Nuclear Quadrupole Resonance (NQR) complemented with Differential Thermal Analysis (DTA) measurements. The first technique is very

useful because the electric field gradient is very sensitive to the crystal structure and dynamic properties can be inferred from the temperature behavior of spin-lattice relaxation time (T_1).

Little information can be found in literature about these compounds. The crystal structures of o-dichlorobenzene (ODCB) [4] and o-difluorobenzene [5] at 223 K and 123 K respectively, have been reported. Also infrared and Raman spectroscopy studies have been reported [6] in o-dichloro, o-chlorobromo and o-dibromobenzene. NQR frequencies of ODCB as a function of temperature, as well as the NQR frequency at two temperatures of o-chlorofluorobenzene (OCFB) and o-chlrobromobenzene (OCBB) have been reported [7–9].

In the present work different solid phases were obtained in OCBB and OCFB depending on the cooling rate. As in p-chloroha-lobenzenes, phases with rigid disorder have been found and the static and dynamic characterization of the different phases has been made.

2. Experimental

The o-chlorohalobenzene samples (o-$C_6H_4Cl_2$, o-C_6H_4ClBr, and o-C_6H_4ClF) used in the experiments were obtained from Sigma-Aldrich (catalog # 240664, B60401, 162302 respectively) and used without further purification. ^{35}Cl NQR measurements were done using a Fourier transform pulse spectrometer with a Tecmag NMRkit II unit and a Macintosh-based real time NMR station. The sample container was a glass cylinder of length 3 cm and diameter 1 cm, closed under vacuum. The NQR spectra were obtained using the nuclear spin-echo Fourier transform mapping

* Corresponding author. Fax: +54 351 4334054.
E-mail address: clyde@famaf.unc.edu.ar (S.C. Pérez).
[1] Fellow of CONICET, Argentina.

spectroscopy (NSEFTMS) method [10,11] with $\pi/2 = 12$ μs. The value of τ was set to 70 μs ($\tau \gg T_2^*$) in order to eliminate distortions from the FID of the second pulse. The mapping frequency step used was 18.6 kHz and the number of scan was 200. The T_1 measurements were made using the standard $\pi/2 - \tau - \pi/2$ two-pulse sequence in ODCB but, upon the echo, in OCBB and OCFB with $\pi/2 = 13$ μs and $\tau = 70$ μs. The temperature was controlled to within 0.1 K using a homemade cryogenic system with a Lakeshore temperature controller. The temperature range covered was between 80 and the melting point of each compound.

DTA was carried out in a properly calibrated homemade system with heating rates of 0.2 K min^{-1}. The sample and reference container are cylinders of length 1 cm and diameter 0.4 cm. The reference sample used was benzoic acid. The DTA records were obtained heating the sample after cooling down the specimen at liquid nitrogen temperature in two different ways: (i) slow cooling at a rate of 0.3 K min^{-1} and (ii) rapid cooling from the liquid state at room temperature down to 77 K by plunging the specimen into liquid nitrogen.

3. Results and discussion

3.1. DTA measurements

Fig. 1a shows a DTA record of OCBB after the sample was slowly cooled from room temperature to liquid nitrogen temperature. Three phase transitions are observed: two endothermic peaks at 183.4 K and at 209.8 K and the fusion at 260.7 K. Therefore, three different crystalline phases exist in the solid. From now on we will call phase III to that existing below 183.4 K, phase II to the solid phase present in the temperature range 184–210 and phase I to that detected above 210 K. When the sample is quenched to liquid nitrogen temperature, no phase transition is observed in DTA record, except for the fusion. This implies that phase I is obtained by rapid cooling fact that is confirmed by NQR. Having in mind the heat-of-transition rule, these polymorphs are enantiotrops.
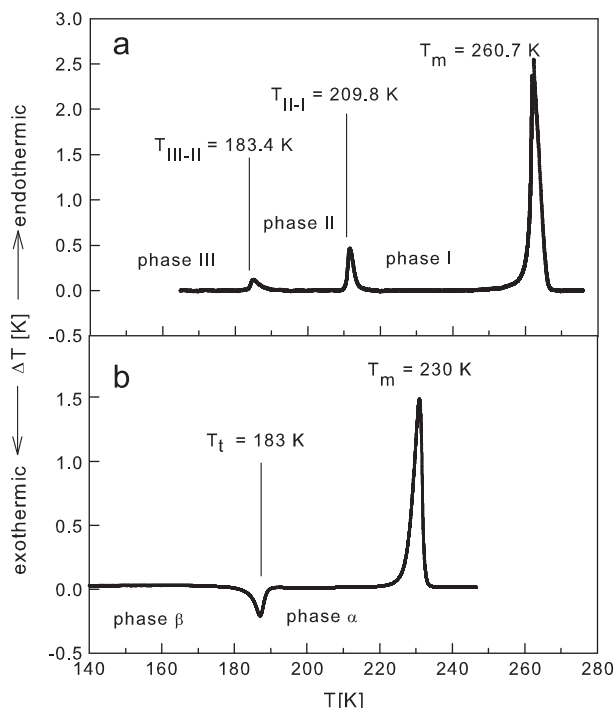
Fig. 1b shows a DTA record of OCFB when the sample was cooled by quenching the liquid phase at 77 K. In this case, only two phase transitions are detected in the whole temperature range (77–250 K): an exothermic peak at 183 K and the fusion at 230 K implying the existence of two crystalline phases. No glass transition was observed within the experimental resolution. The phase that exists below 183 K will be called phase β and the phase above this temperature, phase α. The phase transition observed is monotropic. The DTA record obtained when the sample is cooled to 77 K by slow cooling does not show any phase transition, except for the fusion, which indicates that phase α is undercooled below 183 K.

3.2. NQR frequency and line shape analysis

In order to characterize each of the phases detected by DTA in both compounds, the NQR frequency (ν_Q) and the line shape were measured as a function of temperature.

Fig. 2 shows the spectra that characterize the three different crystalline phases obtained in OCBB when the sample is slowly cooled to liquid nitrogen temperature. For $T < 183.4$ K, the spectrum is characterized by four peaks, well distinguished, inhomogeneously broadened ($\Delta\nu \sim 100$ KHz). Between 184 and 210 K, two lines are observed of about 150 KHz and 100 KHz width each, whereas above 210 K only one inhomogeneously broadened peak, of approximately 125 KHz width, is detected. If the OCBB sample is quenched to liquid nitrogen temperature, phase I is obtained and its spectrum at 80 K is shown, for comparison, in Fig. 2c. It is observed that the line shape at low temperatures looks different from the line shape at high temperatures with a shoulder to the right, but this difference is not related to a phase transition as it
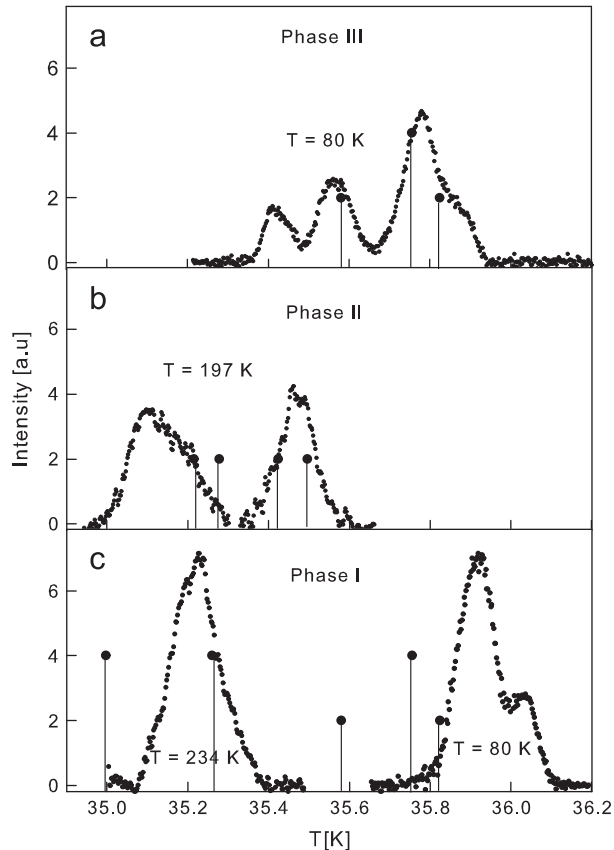
Fig. 1. DTA heating records of (a) OCBB: sample cooled down slowly and (b) OCFB: sample quenched at 77 K.

Fig. 2. NQR line shape of crystalline OCBB (a) below 183 K, (b) between 183 K and 210 K and (c) above 210 K and the same phase at 80 K. The vertical lines represent the NQR frequencies of ordered ODCB.
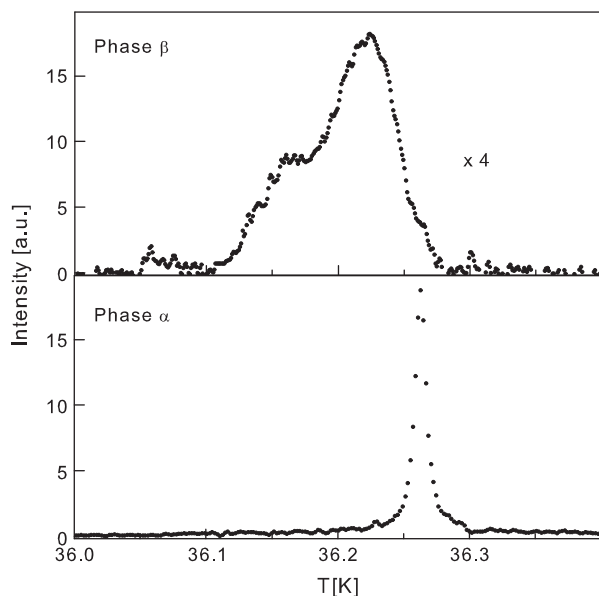
Fig. 3. NQR line shape of crystalline OCFB (a) below 183 K and (b) above 183 K.

Fig. 4. Temperature dependence of the average NQR frequencies. OCFB: ▼ (sample slowly cooled),▽ (sample quenched at 77 K); OCBB: ■ (sample quenched at 77 K), □ (sample slowly cooled) and ODCB: ●.

can be seen from the temperature dependence of ν_Q (see Fig. 4 – full squared)

On the other hand, Fig. 3 shows the line shape that characterizes OCFB when the sample is quenched to liquid nitrogen temperature. Below 183 K, the line is inhomogeneously broadened with a width of the order of 110 KHz, whereas above 183 K the line width is about 20 KHz or less. It is worth noting that the line shape of OCFB in phase β has the same aspect as the line shape of phase I in OCBB but with the shoulder to the left.

The electric field gradient (EFG) at a quadrupole nuclear site is determined by an intramolecular contribution and a crystalline one. The first one is mainly due to the electronic bonding and the second one is due to short-range intermolecular interactions [12]. When orientational disorder is present, a wide distribution of quadrupole frequencies (inhomogeneously broadened line) appears [13–16]. Instead, when order is present, line width of 20 KHz or lower is observed. Therefore in OCBB, because of the line width, it is possible to assume the presence of three disordered phases, while in OCFB one of the phases is disordered (phase β) while the stable phase at high temperatures is an ordered phase (phase α). Once phase α is obtained, it is possible to cool it to 77 K. Since a single resonance frequency is characteristic of this phase, one can assure that there is only one molecule in the asymmetric unit of the crystal structure.

To follow the NQR frequencies behavior with temperature, the center of gravity (average frequency) of the spectra were chosen. The temperature dependence of these frequencies is shown in Fig. 4. The temperature dependence of the center of gravity of ODCB is also included in this figure for the sake of comparison. This compound is characterized by four NQR frequencies of 10 KHz width below 206 K and two frequencies of 10 KHz width above this temperature. These data agree with those reported by Dean and Pound and indicate a solid–solid phase transition at 206 K [7] (see Fig. 7b).

When OCBB is cooled down slowly to 80 K, at a rate of 0.3 K min^{-1} (open square), phase III is obtained and, heating the sample, two jumps are observed in the value of the NQR frequency (at 185 K and at 207 K, approximately) indicating the existence of two phase transitions. The temperatures at which these phase transitions occur are consistent with those observed in DTA record and those reported from Raman and infrared spectroscopy [6]. When OCBB is quenched to liquid nitrogen temperature (full
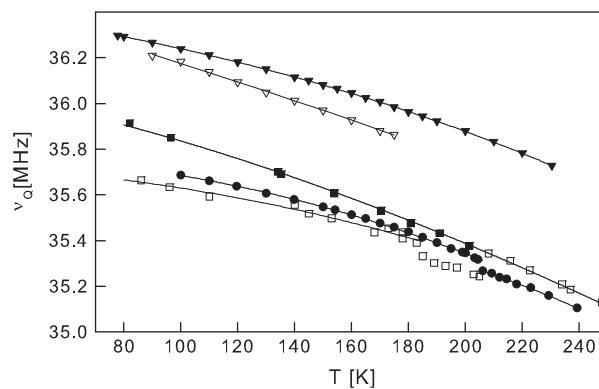
squared) phase I is reached, and no phase transition is observed up to the melting point.

Instead if OCFB is slowly cooled to 77 K (full triangle), phase α is obtained which persists to the fusion, but if the sample is quenched to 77 K, only one phase transition is observed, going up in temperature, at approximatly 180 K in agreement with DTA data. This is a disorder–order phase transition (phase β–phase α).

At first glance, from Fig. 4, it is observed that the temperature dependence of phase III and phase I in OCBB are similar to the temperature dependence of the low and high temperature phases of ODCB respectively.

ODCB crystallizes at high temperature in the space group P2$_1$/n with Z=4 and one molecule in the asymmetric unit [4]. Since the molecule has two chlorine atoms, two NQR frequencies are observed [7]. At low temperatures, there is not crystal structure information but since four NQR frequencies are detected and the molecule has only two chlorines, it is possible to assume that the asymmetric unit has at least two molecules. Therefore, assuming that phase I of OCBB has a structure like that of ODCB at high temperatures, a long-range orientational disorder is necessary to generate a centrosymmetric crystal. In this particular case, one can assume that there is a disordered arrangement of molecules consisting of random occupation of the positions of atoms of chlorine and bromine, a situation that it is present also in p-clorobromobenzene [17,18]. So, the "average molecule" is obtained by the superposition of two molecules with half-weight atoms. Using the fact that the NQR frequency is proportional to the principal component of the EFG, at the chlorine site, along the Cl bond (V_{zz}) [19] and, although no detailed calculation at the nucleus site can be performed, it is possible to obtain the main features of the inhomogeneous spectra with a simple model. In this model, a molecule containing the nucleus of interest is located at the center of a simulated cube consisting of unit cells which reproduce the crystalline array in the compound being studied. The contribution of each neighboring molecule to the principal value of the intermolecular EFG at the chlorine site is calculated as the superposition of point charges located at the atomic positions in the form:

$$V_{zz}^{neighbors} = \sum_i q_i \frac{(3\cos^2\theta_i - 1)}{r_i^3} \qquad (1)$$

where q_i indicates the particular charge assigned to the ith atom of the neighboring molecule and θ_i represents the angle between the radius vector and the direction of the maximum gradient, which approximately coincides with the C–Cl bond. Clearly, charges close to the central chlorine of the simulated cube have the main contribution to the EFG. Furthermore, since the C–H bonds occupy regular lattice sites, the particular charges located at these atoms do

not contribute to the inhomogeneous broadening and can be disregarded for calculations. In this way, only those bonds involving the halogens have to be considered. The point charge assigned to each halogen can be calculated from $p = -(q)d$ where p indicates the dipole moment of the bond and d represents the bond length. Since, as a first order estimate, the molecular dipole results from the superposition of individual dipoles located at each carbon–halogen bond, measured dipole values [20] of monohalobenzenes can be used in Eq. (1). The appropriate bond length can be extracted from those reported by Kitaigorodsky.[21]

The existence of the Sternheimer antishielding effect [19] prevents any absolute numerical comparison between measured and calculated spectra. However, this effect will not depend on the particular configuration of the disordered molecular arrangement and can, in principle, be accounted for by including a multiplicative factor.

In order to reproduce the inhomogeneous NQR profile of phase I in OCBB, the molecule containing the nuclei of interest is located at the center of a simulated cube, with a side length of approximately 170 Å, consisting of monoclinic unit cells which reproduce the P2$_1$/n crystalline array in ODCB and each molecule is allowed to exchange the positions of chlorine and bromine atoms randomly. For each disordered array, the inhomogeneous contribution due to the halogens was calculated at each site the chlorine atom can occupy. About 25000 of these configurations were enough to build smooth profiles which are shown in Fig. 5. The chlorine q_{Cl} was obtained using $p = -(q)d$ and the bromine charge was set proportional to q_{Cl} ($q_{Br} = 1.5 q_{Cl}$). In this way not only the EFG broadening, but also the strain broadening is being considered as proposed by Stoneham [22]. The frequency axis has an arbitrary frequency scale since, as explained above, an absolute comparison is not possible. The main observation to take into account is that each of the two NQR lines of ODCB is split in two lines of same area and approximately same width. This splitting can be explained having in mind that the crystalline contribution to the EFG is mainly due to the closer neighbor charge, that in the disorder proposed can be a Chlorine or a Bromine atom given place to two well distinguished peaks, broadened by the rest of the crystalline contribution. The first neighbor is at $r = 3.57$ Å, while the second ones are at $r = 3.95$ Å.

Using this information, the line shape of phase I in OCBB should be reproduced with four Gaussian lines of same area and width. This is shown in Fig. 6a and b at 80 K and 248 K respectively.

In the same way, if it is assumed that phase III of OCBB is isomorphous with the crystal structure of ODCB in the low temperature phase but with rigid disorder, its spectrum should be well reproduced with eight lines of same area and width. Fig. 6c shows, as an example, a fit of the data at 80 K in phase III, performed under these conditions.
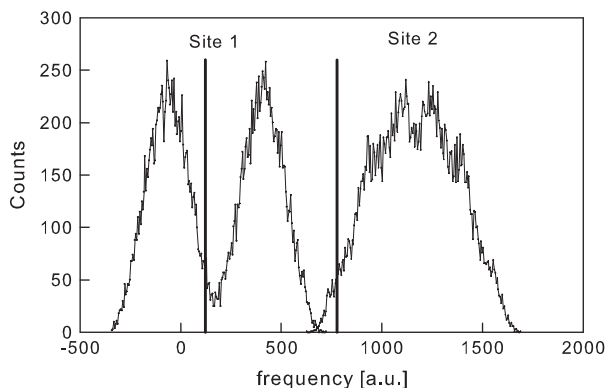

Fig. 5. Distribution, due to disorder, of the intermolecular contribution to the EFG in OCBB at the two crystallographic positions of the Cl atom calculated in the crystalline structure of ODCB at high temperatures. Vertical lines represent the calculated EFG of ordered ODCB.

As it is observed, the fit is quite good in both phases. The line widths of each line are 80 KHz and 115 KHz at 80 K and 248 K, respectively, in phase I and 73 KHz in phase III. Therefore it seems reasonable to assume the existence of the kind of disorder proposed.

A more detailed temperature dependence of ν_Q in phase III of OCBB is shown in Fig. 7a. These NQR frequencies have been obtained from the fit of the NQR spectrum using eight Gaussians of equal area and width. For comparison, the temperature dependence of the four NQR lines of ODCB is also shown (see Fig. 7b). Clearly, in OCBB and in ODCB, there are two characteristic behaviors with temperature. In OCBB, six (there are 2 with equal behavior) of the eight frequencies decrease slower with temperature than the other two lines, while in ODCB three of the four lines have this same dependence. Taking into account that we expect that each line of ODCB splits in two due to disorder, this experimental evidence makes possible to emphasize that phase III in OCBB is isomorphous with the low temperature phase of ODCB.

On the other hand, the fact that the line shape of phase β in OCFB is similar to that of phase I in OCBB makes possible to think also in the presence of a rigid disorder consisting of random occupation of the positions of atoms of chlorine and fluorine in its crystal structure. Actually, its line shape is well fitted with four Gaussians of same area and width (see Fig. 6d). It is worth noting at this point that o-difluorobenzene also crystallizes in a monoclinic P2$_1$/n structure with Z=4 and Z'=1 as ODCB.

The NQR frequency decreases monotonically with temperature due to an average effect of the molecular torsional oscillations in the EFG [23] according to:

$$\nu_Q(T) = \nu_o \left(1 - \frac{3}{2} \langle \theta^2(T) \rangle \right) \qquad (2)$$

where θ is the angular displacement of the z-axis of EFG tensor from its equilibrium position. Experimental data are generally well fitted using the Bayer–Kushida model [24]:

$$\nu_Q(T) = \nu_o \left(1 - \frac{3}{2} \frac{\hbar}{I \omega_t} \coth \left(\frac{\hbar \omega}{2 k_B T} \right) \right) \qquad (3)$$

where ν_o is the limiting static value of the resonance frequency and represents the NQR frequency of a hypothetical rigid lattice. I is an effective moment of inertia [25,26] and $\omega_t = \omega_o(1 - gT)$ is an average torsional frequency, where the anharmonic effects have been taken into account assuming a linear temperature dependence of ω_t [27].

The inverse of the effective moments of inertia calculated geometrically ($1/I$) using the crystallographic molecular data of ODCB and the typical C–F and C–Br bond length are 4.7×10^{-3}, 2.8×10^{-3} and 5.3×10^{-3} (amu Å^2)$^{-1}$ for ODCB, ODBB and OCFB respectively.

A least squared fit of data in phase III of OCBB and in the low temperature phase of ODCB, using Eq. (3) and the geometric moments of inertia listed above, assuming a shared value of g, gives the values reported in Table 1 with a fitted g of 0.0017. Clearly Line 2 in ODCB and Lines 3 and 4 in OCBB have a lower average torsional frequency.

The same analysis can be applied to the high temperature phase of OCBB, ODCB and the disordered phase of OCFB. The results with a fitted g of 0.0004 are also shown in Table 1. In the disordered phase of OCFB, only two frequencies are reported because, as a result of fitting the spectrum with four Gaussians of same area and width, always is obtained a fit like that in Fig. 6d. The parameters of the fit of $\nu_Q(T)$ in phase α of OCFB, with a fitted g of 0.001, are also reported in Table 1.

The values of the average torsional frequencies obtained in OCBB and ODCB are in good agreement with those reported from Raman and Infrared spectroscopy [6]. On the other hand, the
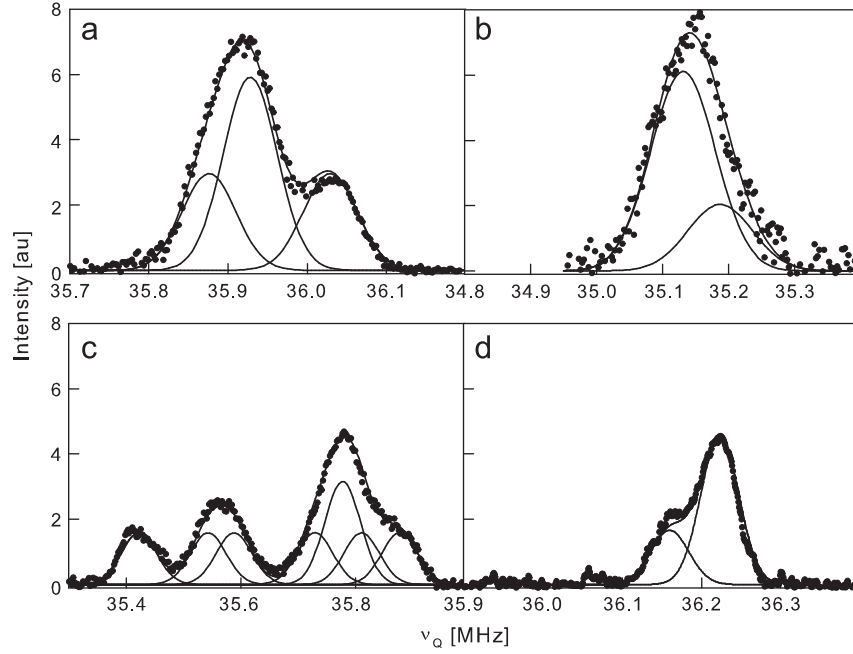
Fig. 6. Fit of NQR spectra with Gaussian functions as explained in the text: (a), (b) phase I of OCBB, (c) phase III of OCBB and (d) phase β of OCFB. (a) Phase I -80k (b) Phase I -248k (c) Phase III -80k (d) Phase β -90k.
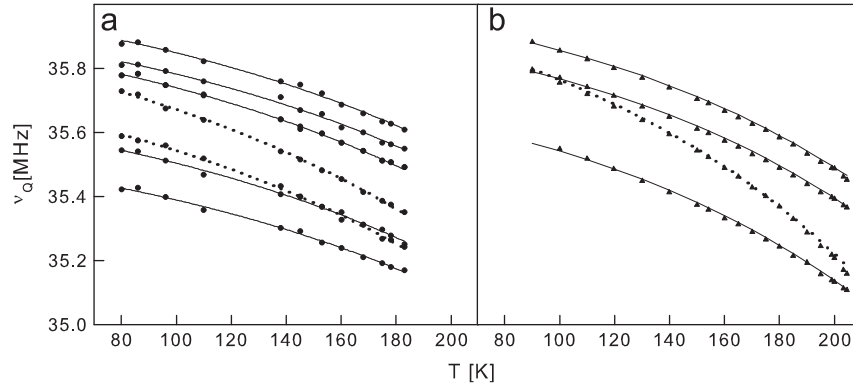

Fig. 7. Temperature dependence of (a) the eight lines obtained from the fit in phase III of OCBB and (b) the four lines in the low temperature phase of ODCB. Solid and dotted lines: fit using Eq. (3).

Table 1
Fitting parameters of $\nu_Q(T)$.

	Phase	Parameter	Line 1	Line 2	Line 3	Line 4	Line 5,6	Line 7	Line 8
OCBB	III	ν_o [MHz]	35.536	35.662	35.738	35.880	35.904	35.935	36.003
		ω_o [cm^{-1}]	60.7	58.5	52.4	50.8	57.4	59.7	59.5
ODCB	LT	ν_o [MHz]	35.698	35.927	35.866	35.935			
		ω_o [cm^{-1}]	74.6	64.7	77.9	78.6			
OCBB	I	ν_o [MHz]	36.186	36.210	36.258	36.353			
		ω_o [cm^{-1}]	32.0	32.4	32.3	31.6			
ODCB	HT	ν_o [MHz]	36.040	36.156					
		ω_o [cm^{-1}]	41.3	44.7					
OCFB	β	ν_o [MHz]	36.518	36.568					
		ω_o [cm^{-1}]	44.0	45.3					
OCFB	α	ν_o [MHz]	36.486						
		ω_o [cm^{-1}]	60						

average torsional frequencies in phase β of OCFB are slightly larger than those of the high temperature phase of ODCB.

If we compare the average torsional frequencies determined in phase III of OCBB with those obtained in the low temperature phase of ODCB we find the ratio $\overline{(\omega_o^{ODCB}/\omega_o^{OCBB})^2} \approx 1.7$. The same ratio, but between phase I of OCBB and the high temperature phase of ODCB, gives 1.8 while the quotient of the inverse of the effective moments of inertia is 1.69. If the comparison is done
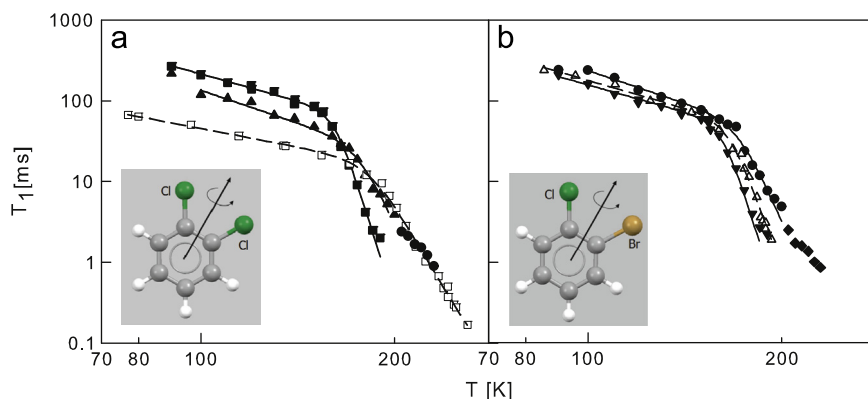
Fig. 8. Temperature dependence of T_1 in ODCB and in OCBB. (a) ■ line 1 LTP ODCB, ▲ line 3 LTP ODCB, □ phase I OCBB and ● line 1 HTP ODCB and (b) ● line 2 LTP ODCB, ▼ line 4 LTP ODCB, △ phase III OCBB and ◆ line 2 HTP ODCB. (- - -) (———) Fit of data using Eq. (4).

Table 2
Fitting parameters of $T_1(T)$.

		λ	τ_o [s]	E [kJ/mol]	q'/q
ODCB LTP	Line 1y 4	2.1	1.2×10^{-13}	37	
	Line 2 y 3	2.6	4.1×10^{-12}	34	
OCBB	Phase III	2.1	2.4×10^{-13}	37	
	Phase I	1.6	$5.5e-10^{-10}$	27	
OCFB	Phase II	2.2	2.6×10^{-12}	7.7	0.0014
	Phase I	2.3			

between phase β of OCFB and the high temperature phase of ODCB, then $(\overline{\omega_o^{ODCB}}/\overline{\omega_o^{OCFB}})^2 \approx 0.93$ and the ratio of the inverse of the effective moments of inertia is 0.89. This is consistent with the Raman work of Bellows and Prasad [28] where they showed that in p-dihalobenzenes with the same packing there is a nearly linear relationship between the square of the rotational phonon modes frequencies and the inverse of average moment of inertia.

3.3. Nuclear quadrupole spin-lattice relaxation time

The temperature dependence of T_1 in the low (LTP) and high temperature phases (HTP) of ODCB are reported in Fig. 8a and b. The relaxation times in intermediate phase II, not shown here, were difficult to measure because the poor signal and their short values, but they have values similar to phase III near the transition temperature to phase II. In the LTP, below 150 K, $T_1(T)$ has a behavior due to torsional oscillations [29] while above this temperature another relaxation mechanism is present, which follows an Arrhenius type behavior, typically found when molecular reorientations take place and quadrupole nucleus belongs to the group that is reorienting [30]:

$$\frac{1}{T_1} = \left(\frac{1}{T_1}\right)_{lib} + \left(\frac{1}{T_1}\right)_{reo} = AT^\lambda + \frac{1}{\tau_o}e^{-E_r/kT} \qquad (4)$$

where E_r is the activation energy. On the other hand, in the HTP of ODCB the relaxation process is clearly dominated by molecular reorientations only.

A least squares fit of data with Eq. (4) gives the parameters shown in Table 2. In the low temperature phase, lines 1 and 4 share the same temperature dependence as well as lines 2 and 3.

To compare the temperature dependence of T_1 in OCBB, T_1 of phase I has been introduced in Fig. 8a and T_1 of phase III has been introduced in Fig. 8b. At first glance is clear that in both phases the low temperature behavior is due to torsional oscillations, while the behavior at high temperature is due to molecular reorientations. Moreover, it is obvious that the dynamical behavior of OCBB
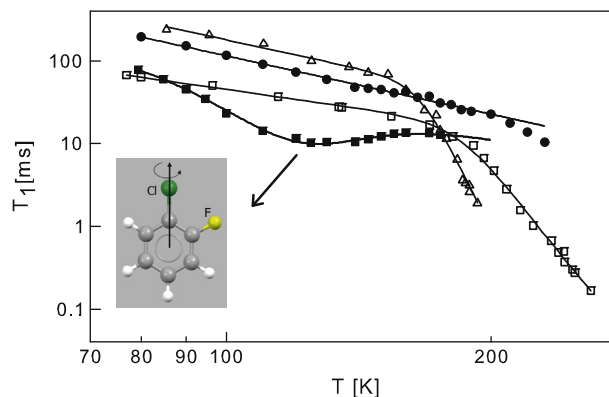

Fig. 9. Temperature dependence of T_1 in OCBB and in OCFB. ● phase α OCFB; ■ phase β OCFB; △ phase III OCBB and □ phase I OCBB. (—) Fit of data using Eqs. (4) and (5).

in phase III is equivalent to that observed in the LTP of ODCB; while the high temperature dependence of OCBB in phase I is similar to that of the HTP of ODCB. This experimental evidence emphasizes the assumption of isomorphism. The parameters of a least squares fit of data with Eq. (4) are also shown in Table 2.

Fig. 9 shows the temperature dependence of T_1 in the ordered phase and the disordered phases of OCFB. $T_1(T)$ in phases III and I of OCBB are also shown for the sake of comparison.

In the ordered phase, T_1 has a behavior due only to torsional oscillations with $\lambda = 2.3$. On the other hand, the temperature dependence of T_1 in the disordered phase (phase β) shows a minimum around 130 K. This behavior is typically observed when the quadrupolar nucleus does not reorient, but its EFG is modulated by molecular reorientations [31]. The only possibility for the existence of EFG modulation is, in this case, a molecular reorientation around an axis that contains the C–Cl bond (pseudo-symmetry axis). In this case:

$$\frac{1}{T_1} = \left(\frac{1}{T_1}\right)_{lib} + \left(\frac{1}{T_1}\right)_{mod} = AT^\lambda + \frac{1}{6}\left(\frac{q'}{q}\right)^2 \frac{\omega_Q^2 \tau}{1+\omega_Q^2 \tau^2} \qquad (5)$$

where (q'/q) and τ denote the fluctuating fraction of the EFG and the correlation time for reorientation of the molecule, respectively. The correlation time τ follows the Arrhenius law $\tau = \tau_o \exp(-E/k_B T)$ where E is the activation energy for this motion. The parameters of a least squares fit of data with Eq. (5) are shown in Table 2

Given that the molecular reorientation can occur only around the pseudo-symmetry axis in OCFB, it is possible to propose that in ODCB and OCBB, the molecular reorientations of chlorine atoms

take place around the molecular symmetry axis and the pseudo-symmetry axis, respectively, as shown in the inset of Fig. 8.

The reorientational dynamics proposed in each compound studied, correspond to reorientations out of the benzene ring plane like occurs in some polysubstituted benzenes [32]. The obtained activation energies for this type of reorientation in ODCB and OCBB are higher than those corresponding to molecular reorientations in the plane of the benzene ring observed in p-chloroiodobenzene (31.7 KJ/mol) [33], p-chlrofluorobenzene (21.5 KJ/mol) [34] and pentafluorochorobenzene (21.8 KJ/mol) [35], but of the same order than those obtained in p-chlronitrobenzene (35.5 KJ/mol) and p-chlrobromobenzene (38.5 KJ/mol) [36]. It is not possible a comparison in the case of OCFB.

4. Conclusions

Different polymorphs have been found in o-chlrohalobenzenes. Based in the NQR lineshape analysis, the three solid phases found in OCBB are orientationally disordered, showing an interesting case of polymorphism, while in OCFB only one of the two phases found is disordered.

The detailed study of the temperature dependence of ν_Q and the lineshape analysis, led to propose that the disorder could be explained, in the same way as p-chlrohalobenzenes, with a random occupation of the X (Br, F) and Cl sites in the crystal lattice of o-dichlorobenzene.

Moreover, the analysis of $T_1(T)$ data show that the librational dynamics, as well as the molecular reorientational dynamics, is the same in the low and high temperature phases of OCBB as in ODCB. Based on these facts it is possible to propose that the low and high temperatures phases of OCBB are isomorphous with the low and high temperatures phases of ODCB, a behavior already observed in the p-chlorohalobenzene family.

On the other hand the ordered phase of OCFB is not isomorphous with neither of the ODCB phases, but the disordered phase of this compound may be compatible with the crystal structure of high temperature phase of ODCB, based on lineshape features and $\nu_Q(T)$ analysis. However, the reorientational dynamics is not the same. Due to the fact that no glass transition, upon quenching, has been observed in the DTA record, it is not possible to propose that this disordered phase is an orientational glass, as it has been observed in others compounds like 2-chlorothiophene and 3-chlorothiophene [37–39] where reorientations in plane and out of plane have also been detected. Besides, with the correlations times estimated for out of plane reorientations, the glass transition should be observed below 77 K.

Particularly, in ODCB and OCBB the reorientation involve the Cl nuclei and is around the symmetric and seudo-symmetric molecular axis with activation energies in the range 27–37 KJ/mol. Instead, in OCFB the reorientation does not involve the Cl nucleus and for this reason the reorientation takes place around the pseudo-symmetry axis that contains the C–Cl bond with an activation energy of the order of 7.7 KJ/mol.

References

[1] P.N. Prassat, E.D. Stevena, J. Chem. Phys. 66 (1977) 862.
[2] J.C. Bellws, N. Prassat, J. Chem. Phys. 66 (1977) 625.
[3] P.N. Prassat, R. Von Smith, J. Chem. Phys. 71 (1979) 4646.
[4] R. Boese, M.T. Kirchner, J.D. Dunitz, G. Filippini, A. Gavezzotti, Helv. Chim. Acta 84 (2001) 1561.
[5] V.R. Thalladi, H.C. Weiss, D. Blaser, R. Boese, A. Nangia, G.R. Desirajo, J. Am. Chem. Soc. 120 (1998) 8702.
[6] B. Wyncke, F. Brehat, A. Hadni, Can. J. Chem. 56 (1978) 1638.
[7] C. Dean, R.V. Pound, J. Chem. Phys. 20 (1952) 195.
[8] T.A. Babushkina, V.I. Robas, G.K. Semin, Radio Spektrosk. Tverd. Tela Dokl. Vses. Soveshch. (1967) 221.
[9] W. Pies, A. Weiss, Z. Phys. Chem. 127 (1981) 147.
[10] Y. Tong, J. Mag. Res. A 119 (1996) 22.
[11] A. Bussandri, M. Zuriaga, J. Magn. Res. 131 (1998) 224.
[12] T.P. Das, E.L. Hahn, Nuclear Quadrupole Resonance Spectroscopy, Solid State Physics Supp. 1, Academic, New York, 1958.
[13] C. Meriles, S. Pérez, A.H. Brunetti, Phys. Rev. B 54 (10) (1996) 7090.
[14] C.A. Meriles, S. Pérez, A.H. Brunetti, J. Chem. Phys. 107 (6) (1997) 1753.
[15] C.A. Meriles, S. Pérez, A. Wolfenson, A.H. Brunetti, J. Chem. Phys. 110 (1999) 7392.
[16] N. Veglio, M.J. Zuriaga, G.A. Monti, J. Phys.: Condens. Matter 16 (2004) 7873.
[17] C.A Meriles, R.H. de Almeida Santos, M.T. do Prado Gambardella, J. Ellena, Y.P. Mascarenhas, A.H. Brunetti, J. Mol. Struct. 513 (1999) 245.
[18] A. Maiga, Nguyen-Ba-Chanh, Y. Haget, M.A Cuevas-Diarte, J. Appl. Crystallogr. 17 (1984) 210.
[19] C.P. Slitchter, Principles of magnetic resonance, Springer Series in Solid-State Science, vol. 1, Third Enlarged and Updated Edition, 1990.
[20] Landolt-Bornstein, Zahlenwerte und Funktionen, I Band Atom und Molekular Physik, 3 teil, Springer-Verlag, Berlin, 1951.
[21] A.J. Pertsin, A.I. Kitaigorodsky, The Atom–Atom Potential Method, Springer-Verlag, Berlin, 1987.
[22] A.M. Stoneham, Rev. Mod. Phys. 41 (1969) 82.
[23] H. Bayer, Z. Phys. 130 (1951) 227.
[24] H. Chihara, N. Nakamura, Advances in Nuclear Quadrupole Resonance, Vol 4, Heyden, London, 1980.
[25] M. Zuriaga, G. Monti, C. Martin, J. Phys.: Condens. Matter 3 (1991) 2287.
[26] R.N. Hasting, T. Oja, J. Chem. Phys. 57 (1972) 2139.
[27] R.J.C. Brown, J. Chem. Phys. 32 (1960) 116.
[28] J.C. Bellows, P.N. Prasad, J. Chem. Phys. 66 (1977) 625.
[29] L.V. Jones, M. Sabir, J.A.S. Smith, J. Phys. C 11 (1978) 4077.
[30] S. Alexander, A. Tzalmona, Phys. Rev. A 138 (1965) 845.
[31] D.E. Woessner, H.S. Gutowsky, J. Chem. Phys. 39 (1963) 340.
[32] A.I. Rubailo, S.P. Gabuda, V.E. Volkov, J. Struct. Chem. 10 (4) (1969) 635.
[33] C.A. Meriles, S.C. Pérez, A.E. Wolfenson, A.H. Brunetti, J. Chem. Phys. 110 (15) (1999) 7392.
[34] L. Cerioni, S. Pérez, A. Wolfenson, J. Phys. Chem. Solids 65 (2004) 1133.
[35] N.E. Ainbinder, G.E. Kibrik, A.N. Osipenko, G.B. Soifer, Phys. Solid State 39 (5) (1997) 780.
[36] C.A. Meriles, S.C. Pérez, A.H. Brunetti, J. Chem. Phys. 107 (6) (1997) 1753.
[37] H. Fujimori, T. Asaji, Z. Naturforsch. 55a (2000) 183.
[38] H. Fujimori, A. Todoroki, T. Asaji, M. Oguni, AIP Conf. Proc 708 (2004) 685.
[39] H. Fujimori, T. Kaneko, T. Asaji, Hyperfine. Interact. 181 (2008) 87.